Vibrational Energy Distributions through Kinetic Analysis. Early Collisional Relaxation of T_1 Pyrazine

Derek R. McDowell,† Fei Wu, and R. Bruce Weisman*

Department of Chemistry and Rice Quantum Institute, Rice University, Houston, Texas 77005

Received: April 24, 1997; In Final Form: June 2, 1997[⊗]

A new kinetics-based method is described for determining the distribution of vibrational energy contents in a highly excited, precollisional polyatomic sample. The method can be applied to excited species whose population decay constant depends on vibrational energy. In such cases a sample's decay kinetics will show a distribution of rate constants corresponding to the underlying initial distribution of vibrational energies. This method is illustrated using low-pressure pyrazine samples whose total T_1 population is measured by triplet−triplet transient absorption and kinetically analyzed to obtain a decay constant distribution modeled as a sum of Gaussian peaks. The result is then transformed into a vibrational energy distribution using an independently determined calibration curve. The sample's relatively narrow nascent energy distribution appears to evolve into a bimodal form through collisions with helium atoms. It is estimated that approximately 0.7% (on average) of the gas kinetic encounters between an excited triplet pyrazine molecule and a helium atom lead to vibrational deactivation of *ca*. 2000 cm^{-1}.

Introduction

It has long been recognized that vibrational excitation in polyatomic molecules can play a controlling role in their kinetic and dynamic behavior. Within the past 15 years, our knowledge of collisional energy transfer in highly excited systems has been greatly enhanced by the introduction of "direct" methods that reveal average vibrational energy contents during relaxation. A more informative but highly elusive quantity is a sample's full vibrational energy distribution, whose changing first moment is measured by the direct methods. Recently, more detailed infrared emission experiments have provided both the first and second moments of the energy distribution for some relaxing polyatomics.[1,2] In addition, the KCSI energy-selected photoionization technique of Luther and co-workers[3] reveals energy distributions during the approach to thermalization.

We report here a new method for deducing precollisional vibrational energy distributions from kinetic analysis ("VEDKA"). This VEDKA method may be applied to excited species whose population decay constant varies with vibrational energy content. In such systems, an inhomogeneous distribution of energy contents among sample molecules leads to overall population kinetics showing a superposition of differing decay constants. If reliable kinetic data can be measured on an unperturbed sample, an appropriate analysis can extract that distribution of decay constants. Then, given the quantitative relation between decay constant and vibrational energy content, one can transform the deduced distribution of sample decay constants to reveal the underlying distribution of vibrational energies.

We illustrate this method with studies of low-pressure pyrazine vapor that has been optically excited to selected vibronic levels of the S_1 state. Subnanosecond $S_1 \rightarrow T_1$ intersystem crossing quickly converts the excited pyrazine molecules into vibrationally excited triplet states. We monitor the presence of these triplets through induced absorption measurements within a diffuse $T_n \leftarrow T_1$ system in which the triplet's molar absorptivity varies only mildly with vibrational excitation. We can therefore determine the time-dependent total triplet population using a single probe wavelength. The triplet pyrazine population decays almost exclusively by $T_1 \rightarrow S_0$ intersystem crossing with a rate constant that depends strongly on vibrational energy content. Because of this dependence, the measured decay kinetics contain information about the distribution of sample vibrational energies. Analysis of our data confirms that the nascent vibrational energy distribution among the pyrazine triplets is relatively narrow. In addition, we find evidence for a surprisingly efficient relaxation channel that converts the distribution into a bimodal form through collisions with helium.

Experimental Section

Static samples of pyrazine vapor are contained in a 68 cm optical cell connected to a capacitance manometer (MKS model 120-AA). Tunable ultraviolet pulses from a Q-switched Nd:YAG/dye laser system pass through the sample cell, exciting pyrazine's 0_0^0 or $8a_0^1$ vibronic transition to give triplet vibrational energy contents of 4056 or 5433 cm^{-1}, respectively. Triplet−triplet absorption is monitored through attenuation of a continuous probing beam from a 676 nm diode laser (PTI Model ACM15). This beam crosses the excitation axis at a small angle in order to avoid spurious signals from the cell windows. The probe beam's time-dependent intensity is detected by a filtered and baffled photoconductive silicon photodiode whose output is recorded by a Tektronix TDS-744A digitizing oscilloscope. The oscilloscope is used in bandwidth-limited mode, with an input impedance of 240 or 50 Ω. Waveforms averaged over several thousand excitation pulses are transferred from the oscilloscope to a laboratory computer for conversion into induced absorbance and further analysis. The time response function of this instrument is determined by directing a small portion of the excitation beam onto the probe detector and recording the resulting pulse shape under the same detection conditions normally used for acquiring induced absorption data. The resulting response function, whose width at half-maximum is approximately 28 ns with 240 Ω termination, likely contains errors at the 1% level arising from a slight

† Present address: Dept. of Chemistry, Wittenberg University, P.O. Box 720, Springfield, OH 45501.

⊗ Abstract published in *Advance ACS Abstracts,* July 1, 1997.

S1089-5639(97)01377-7 CCC: $14.00

wavelength-dependence of the detector's rise time. Scans taken on empty sample cells show systematic and random absorbance errors below *ca.* 2×10^{-6}, giving signal-to-root-mean-square-noise ratios of several hundred at the peak. No smoothing or other postfiltering is applied to the data.

Data Analysis

Data analysis begins by defining $f_E(E,t)$, a time-dependent function that describes the inhomogeneous distribution of vibrational energies in the triplet population and whose integral equals the total T_1 population at time t. Because the $T_n \leftarrow T_1$ spectrum probed in this experiment is broad and diffuse, triplet sample molecules in all stages of vibrational relaxation contribute to the induced absorption signal, although with somewhat varying strengths represented by an energy-dependent absorption cross section function, $\sigma(E)$. Each differential energy range therefore contributes an absorption signal $\sigma(E)\, f_E(E,t)\, \mathrm{d}E$, giving a total measured signal

$$S(t) \propto \int_0^\infty \sigma(E)\, f_E(E,t)\, \mathrm{d}E \tag{1}$$

Triplet sample molecules decay with first-order rate constants that increase monotonically with their vibrational energy content, a dependence expressed by the "calibration" function $k(E)$. The population distribution function $f_E(E,t)$, can change through two processes: (1) collisional transfer of population among the energy components; (2) first-order decay of each isolated energy component.

In the limit of pressures low enough that the first process may be neglected relative to the second, each energy component undergoes an independent exponential decay:

$$f_E(E,t) = \mathrm{e}^{-k(E)t}\, f_E(E,0) \tag{2}$$

This leads to a measured time-dependent signal of the form

$$S(t) \propto \int_0^\infty \mathrm{e}^{-k(E)t}\, f'_E(E,0)\, \mathrm{d}E \tag{3}$$

where $f'_E(E,t)$, denotes the sensitivity-weighted energy distribution function $\sigma(E)\, f_E(E,t)$. If all molecules in a low-pressure sample have the same energy, then the observed signal will show simple exponential decay with a rate constant corresponding to that energy. On the other hand, a broadened energy distribution will give a signal composed of a superposition of exponential decays.

Experimentally, one can analyze low-pressure kinetic data to find the initial rate constant distribution function, $f_k(k,0)$, through the expression

$$S(t) \propto \int_0^\infty \mathrm{e}^{-kt}\, f_k(k,0)\, \mathrm{d}k \tag{4}$$

Once found, the nascent $f_k(k)$ may be transformed into the corresponding energy distribution function, $f'_E(E,)$, using the "calibration" function, $k(E)$, its inverse, $E(k)$, and the following relation:

$$f'_E(E(k)) = f_k(k)\frac{\mathrm{d}k}{\mathrm{d}E} \tag{5}$$

Rate constant distributions may be extracted from kinetic data through inverse Laplace transform approaches such as CONTIN[4−6] or through the maximum entropy method.[7] However, because Gaussian distributions are both mathematically tractable and also commonly observed in trajectory and master equation simulations of vibrational relaxation,[1,8,9] we have instead chosen to model the decay constant distributions as sums

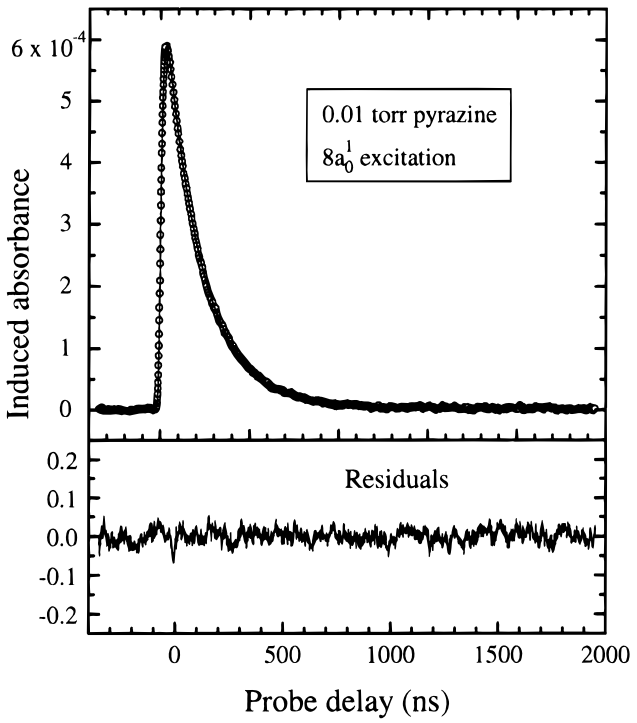

Figure 1. Induced absorbance measured at 676 nm after excitation of a sample containing 0.01 Torr of pyrazine. (top) Data (open circles) and fit (solid curve) computed as described in the text. (bottom) Difference between data and fit.

of Gaussian peaks. In our model, each peak has an independent center position k_i, width parameter σ_i and amplitude A_i:

$$f(k) = \sum_{\text{peaks } i} \frac{A_i}{\sqrt{2\pi}\,\sigma_i}\, \mathrm{e}^{(-1/2)((k-k_i)/\sigma_i)^2} \tag{6}$$

The A_i values are scaled so that they sum to one. This model reduces to a familiar sum of exponential decays in the limit of peak widths that are small relative to their center frequencies. In our analysis program, a Marquardt nonlinear fitting routine[10] iteratively adjusts the Gaussian parameters to achieve the best least-squares match between an experimental kinetic trace and the convolution of the simulated *S(t)* with our measured instrument response function. We find that two or three peaks are typically needed to generate an accurate fit to the data and that the deduced parameters are independent of oscilloscope input impedance.

Results and Discussion

Near-Nascent Conditions. Figure 1 shows induced absorbance data measured following $8a_0^1$ excitation of a pyrazine sample at 0.01 Torr, at which pressure the mean Lennard-Jones collision interval is 4.4 μs, or 22 times the nascent triplet lifetime. In the figure's upper frame, data points are shown as open circles and the optimized fit, based on eq 6 with $i = 3$, is drawn as a solid line. The lower frame displays the difference between data and fit on an expanded absorbance scale. These residuals have a root-mean-square value of 1.7×10^{-6}, significantly lower than obtained by fitting to a sum of three simple exponentials. The $f(k)$ distribution that corresponds to the fit in Figure 1 is presented in Figure 2, except for a small high-frequency component, centered near $21 \times 10^6\ \mathrm{s}^{-1}$, whose size and position depend sensitively on the exact shape of the instrumental response function. It seems likely that this peak is an artifact arising from a small systematic error in our determination of that function.

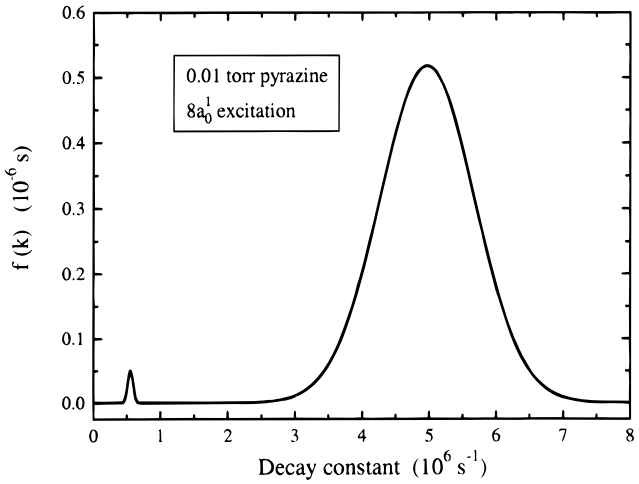

Figure 2. Decay constant distribution function corresponding to the fit of Figure 1.

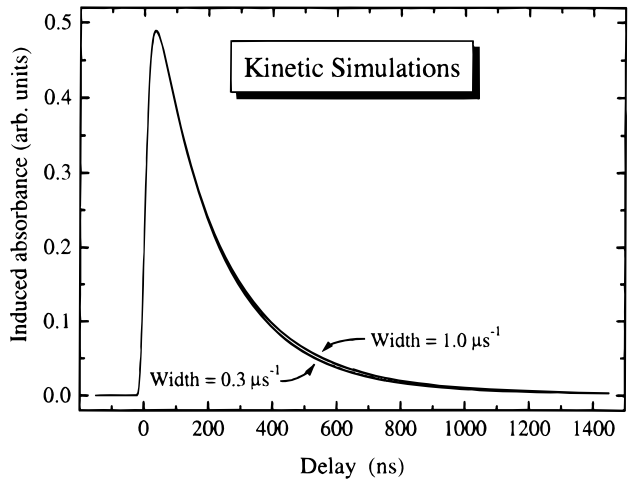

Figure 3. Simulated kinetic data illustrating the effect of the main peak's width parameter (σ) on the kinetic trace. Other parameters match those of the fit in Figure 1.

The dominant feature in Figure 2, centered at 5.0×10^6 s^{-1}, corresponds to $T_1 \rightarrow S_0$ radiationless decay of the nearly nascent triplet pyrazine molecules prepared with 5433 cm^{-1} of vibrational energy. An important question is how meaningfully the width of this peak can be deduced through analysis of actual experimental data. To show the sensitivity of the kinetic shape to the main peak's width, we display in Figure 3 synthetic kinetic traces computed from parameters similar to those used in Figure 2. For delays near 450 ns, traces with main peak widths of 0.3 and 1.0×10^6 s^{-1} differ by approximately 1% of the maximum value. Although this difference is surely minor, it can be readily resolved in data having the precision shown in Figure 1. From our analyses we find the main peak width to be $(0.7 \pm 0.2) \times 10^6$ s^{-1}. Figure 2 also shows a small decay component near 0.5×10^6 s^{-1} whose integrated population is *ca*. 0.5% of the main peak's (too small to allow width determination). This secondary peak appears to result from collisional relaxation by ground state pyrazine molecules in a process similar to the helium-induced relaxation discussed below.

Following the data fitting, we use eq 5 to transform the deduced decay rate distribution into its vibrational energy distribution, shown in the top frame of Figure 4. For comparison, the bottom frame of Figure 4 displays the energy distribution calculated for a thermal triplet pyrazine sample (at 841 K) whose average vibrational energy equals the nascent sample's. (The corresponding thermal distribution near 300 K has large irregularities that reflect discontinuities in the density of states

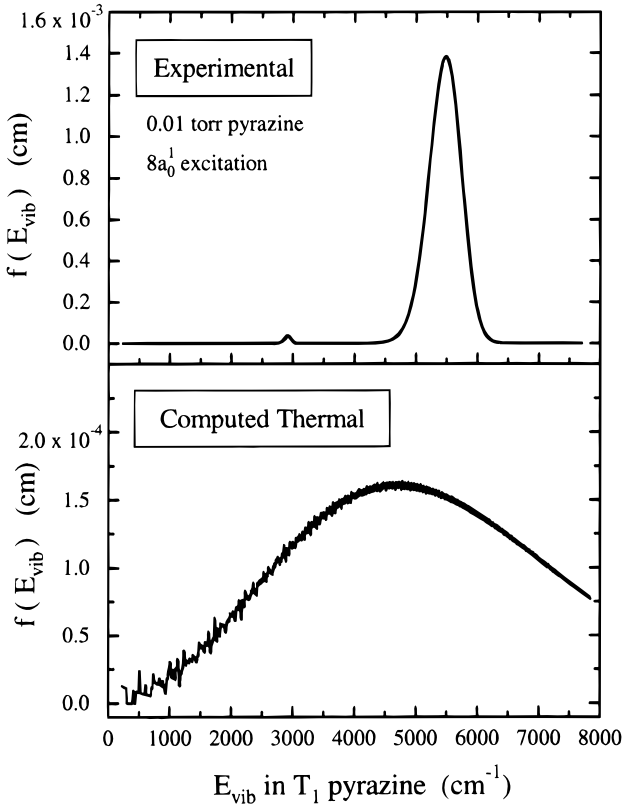

Figure 4. (top) Vibrational energy distribution function deduced from the decay constant distribution function of Figure 2. (bottom) Calculated vibrational energy distribution function for a T_1 pyrazine sample thermally equilibrated at 841 K (giving the same average energy as provided by $8a_0^1$ excitation).

function at low energies; its "width" is roughly comparable to the main peak's in the top frame.) In performing these calculations we used the set of triplet vibrational frequencies compiled earlier,[11] corrected with the recent spectroscopic analysis of Fisher.[12] The far narrower distribution in the top frame compared to the bottom qualitatively confirms our expectation of a well-defined nascent energy distribution.

Effects of Early Collisions. Although the analysis described above is rigorously valid only in the precollisional limit, it may also prove useful for revealing the effects of the earliest collisions. We have therefore performed decay rate distribution analyses for samples containing 0.01 Torr of pyrazine plus small pressures of added helium. In this series of measurements we excited the sample at the more intense 0_0^0 transition in order to enhance the signal strength. (This longer excitation wavelength lowers the initial triplet energy to $E_{vib} = 4056$ cm^{-1}, slowing the nascent decay constant to 2×10^6 s^{-1}.) As seen in Figure 5, two effects of the added helium are apparent. First, the nascent, dominant peak near 2×10^6 s^{-1} is significantly broadened. We attribute this broadening to cascade relaxation processes in which components of the triplet energy distribution are collisionally interconverted before completing their independent radiationless decays. The second apparent effect is growth of the low-frequency peak near 0.15×10^6 s^{-1}, which, according to our knowledge of $k(E)$, corresponds to triplet pyrazine molecules that have lost approximately 2000 cm^{-1} of vibrational energy. This partially relaxed population evidently arises from efficient V $\rightarrow$ T, R processes in collisions with helium. As for why population accumulates near 2000 cm^{-1}, we note that this energy matches the threshold in relaxation susceptibility found in previous studies of triplet pyrazine's energy-dependent collisional energy loss.[11,13−15] Excited triplet molecules can therefore undergo efficient relaxation until their energy content approaches 2000 cm^{-1}, after which they become

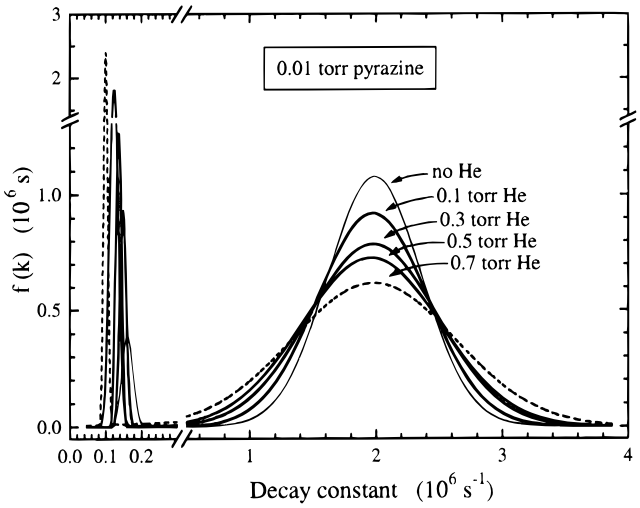

Figure 5. Decay constant distributions derived from pyrazine samples excited at 0_0^0 in the presence of various pressures of helium buffer gas.

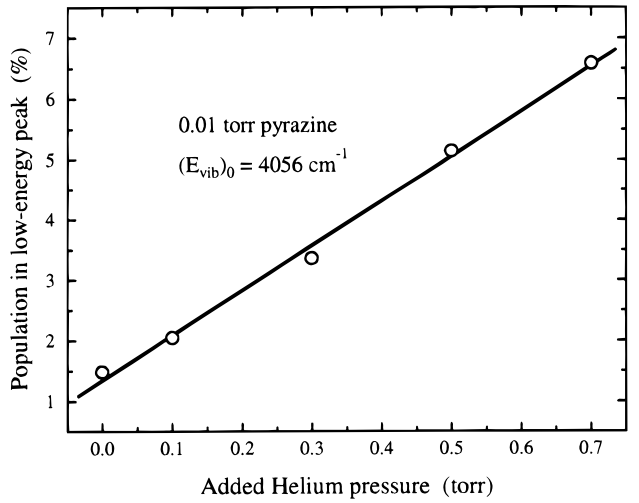

Figure 6. Population percentage represented by the low-frequency peak in Figure 4 as a function of the added helium pressure.

relatively resistant to further relaxation. This results in a kinetic bottleneck and a temporary bimodal energy distribution function. We note that bimodal forms would likely remain hidden from experimental methods that deduce only two or three moments of the energy distribution.

Figure 6 plots the variation of the slow-decaying peak's integral as a function of helium pressure. The slope of the data implies a significant probability for removal of approximately half of the vibrational energy of T_1 pyrazine donor molecules by collisions with helium atoms. To estimate the rate constant for this surprising relaxation process, we have used a simplified kinetic cascade model containing only three species: the nascent triplet pyrazine (with 4056 cm^{-1} of vibrational energy), partially relaxed triplet pyrazine (with *ca*. 2000 cm^{-1} of vibrational energy), and ground electronic state pyrazine (invisible at our probing wavelength). In this model, the two triplet species are assigned appropriate rate constants for unimolecular decay to the ground state, and collisional conversion of the nascent triplet into the partially relaxed form is described by a bimolecular rate constant. Adjustment of the parameters in this simple model allows very good fits to measured kinetic traces. From the optimized parameter values obtained for several helium pressures, we deduce the bimolecular rate constant for partial vibrational relaxation to be 1.3×10^5 s^{-1} $Torr^{-1}$, or 0.7% of the gas kinetic encounter rate between helium and pyrazine. We believe that this result is semiquantitatively valid despite the simplicity of the model used to obtain it. The efficiency deduced for this 2000 cm^{-1} V → T, R "supercollision" process is far larger than expected from relaxation studies of pyrazine in its ground electronic state.[16] This difference suggests a mechanism involving properties peculiar to the electronically excited state of the donor. Nevertheless, our deduced relaxation efficiency lies at least 2 orders of magnitude below that for fluorescence quenching in pyrazine,[17] confirming the distinction between these two processes. In interpreting our result one should note that individual collision intervals can be much shorter than the mean value, triplet Lennard-Jones parameters may exceed the ground state values assumed in this estimate, and Lennard-Jones parameters may underestimate relaxation cross sections in general.

Conclusion

In summary, we have shown that the VEDKA method allows near-nascent vibrational energy distributions to be deduced from kinetic data taken under low-pressure conditions. The energy distribution of T_1 pyrazine formed through intersystem crossing is confirmed to be much narrower than a thermal distribution. This method loses validity at pressures high enough to give significant collisional changes in energy level populations during the observation period. A proper analysis of pressure-dependent decay rate distributions therefore requires modeling through master equation methods. Even without such detailed modeling, however, our results strongly suggest the rapid formation of a bimodal energy distribution through collisions of triplet pyrazine with helium, the mildest relaxer species.[11,15] The rate of strong deactivation is remarkably high: an average of 0.7% of gas kinetic collisions with helium atoms remove *ca*. 2000 cm^{-1} of vibrational energy from the triplet pyrazine. We believe that with future refinements, the method of high-definition kinetic analysis should prove a powerful tool for investigating the early stages of collisional vibrational relaxation in excited polyatomics.

Acknowledgment. We are grateful to Dr. Michael Barnes for introducing us to kinetic distribution analysis and to the National Science Foundation and the Robert A. Welch Foundation for support of this research.

References and Notes

(1) Brenner, J. D.; Erinjeri, J. P.; Barker, J. R. *Chem. Phys.* **1993**, *175*, 99.
(2) Hartland, G. V.; Quin, D.; Dai, H.-L. *J. Chem. Phys.* **1994**, *100*, 7832.
(3) Lohmannsroben, H. G.; Luther, K. *Chem. Phys. Lett.* **1988**, *144*, 473.
(4) Provencher, S. W. *Comput. Phys. Commun.* **1982**, *27*, 213.
(5) Provencher, S. W. *Comput. Phys. Commun.* **1982**, *27*, 229.
(6) Gregory, R. B.; Zhu, Y. *Nucl. Instrum. Methods* **1990**, *A290*, 172.
(7) Livesey, A. K.; Brochon, J. C. *Biophys. J.* **1987**, *52*, 693.
(8) Troe, J. *J. Chem. Phys.* **1982**, *77*, 3485.
(9) Lendvay, G.; Schatz, G. C. *J. Phys. Chem.* **1990**, *94*, 8864.
(10) Bevington, P. R.; Robinson, D. K. *Data Reduction and Error Analysis for the Physical Sciences*, 2nd ed.; McGraw-Hill: New York, 1992.
(11) Bevilacqua, T. J.; Weisman, R. B. *J. Chem. Phys.* **1993**, *98*, 6316.
(12) Fischer, G. *Can. J. Chem.* **1993**, *71*, 1537.
(13) Bevilacqua, T. J.; Andrews, B. K.; Stout, J. E.; Weisman, R. B. *J. Chem. Phys.* **1990**, *92*, 4627.
(14) Weisman, R. B. Vibrational energy loss from triplet state polyatomics. In *Advances in Chemical Kinetics and Dynamics*; Barker, J. R., Ed.; JAI Press: Greenwich, CT, 1995; Vol. 2B, p 333.
(15) McDowell, D. R.; Weisman, R. B. To be published.
(16) Miller, L. A.; Barker, J. R. *J. Chem. Phys.* **1996**, *105*, 1383.
(17) McDonald, D. B.; Fleming, G. R.; Rice, S. A. *Chem. Phys.* **1981**, *60*, 335.